Transparency and imaginary colors

Transparency and Imaginary Colors

Whitman Richards[1,*], Jan J. Koenderink[2]& Andrea van Doorn[3]

[1]Mass. Institute of Technology, 32-364, Cambridge, MA 02139, USA

[2]Delft University of Technology, Faculty of EEMCS Mekelweg 4, 2628 CD Delft, &

Utrecht University, Dept. Physics & Astronomy, Princetonplein 5 3584 CC Utrecht

The Netherlands

[3]Delft University of Technology, Faculty of Industrial Design

Landbergstraat 15, 2628 CE Delft, The Netherlands

[*]Corresponding author: wrichards@mit.edu

Abstract: Unlike the Metelli monochrome transparencies, when overlays and their backgrounds have chromatic content, the inferred surface colors may not always be physically realizable. In these cases, the inferred chromatic transmittance or reflectance of the overlay is imaginary, lying outside the RGB spectral boundaries. Using the classical Metelli configuration, we demonstrate this illusion, and briefly explore some of its attributes. Some observer differences in perceiving transparencies are also highlighted. These results show that the perception of transparency is much more complex than conventionally envisioned.

OCIS codes: 330.0330,, 330.5020, 330.5510, 330.7310, 350.2450, 290.7050

- Figure 1 about here –

1. Introduction

An imaginary color is a surface color seen as physically realizable in the observed context, but one that is not realizable by accepted physical models. Our simple example is the perception of reflectance (or transmittance) of a uniform surface overlaying a two-panel background, each with different reflectance. To illustrate, P and Q in Fig. 1 are seen by most observers as colors of a single homogeneous transparent surface that overlays two opaque surfaces A and B of different reflectance. In fact, the physical constraints for this interpretation are not satisfied.

Two obvious parameters constraining physical transparency are the reflectance α_λ and the transmittance τ_λ of the overlay. Both must lie in the interval [0, 1]. Using a rotating sectored disc (an episcotister) Metelli [1-3] proposed a simple linear model where the fraction τ_λ of the light from the background was transmitted through an overlay, and the remaining fraction $(1-\tau_\lambda)$ was reflected off the overlay. Hence if P_λ, Q_λ are the two regions of the overlay, and if the two background regions are A_λ, B_λ as shown in Fig. 1, then the observed colors will be

$$P_\lambda = \tau_\lambda A_\lambda + (1-\tau_\lambda)\alpha_\lambda \quad (1a)$$

$$Q_\lambda = \tau_\lambda B_\lambda + (1-\tau_\lambda)\alpha_\lambda \quad (1b).$$

These conditions lead to the following two constraints on relations between the observed components of the background A_λ, B_λ and the overlay P_λ, Q_λ,

$$(0 < \tau_\lambda < 1) \Rightarrow 0 < (P_\lambda - Q_\lambda)/(A_\lambda - B_\lambda) < 1 \quad (2)$$

$$(0 < \alpha_\lambda < 1) \Rightarrow 0 < (-P_\lambda B_\lambda + A_\lambda Q_\lambda)/(A_\lambda - B_\lambda - P_\lambda + Q_\lambda) < 1. \quad (3)$$

Henceforth we will eliminate the λ subscripts, it being understood that conditions (2) and (3) will be checked for all three R, G, B spectral channels used to generate the displays. These formulas completely describe the physics (but see Appendix B for qualifiers.)

- Figure 2 about here -

Because the Metelli model simply adds some fraction of light from the background with that reflected off the overlay, the chromaticity of P must lie on a line from the inferred RGB values of the overlay to the RGB values of its background, namely A, and similarly for B and Q. This condition is illustrated in a depiction of an RGB chromaticity plot in the right panel of Fig 2. The intersection V of these two loci is the expected observed chromaticity, which in this case lies within the spectral boundary and hence is physically plausible. In contrast, the left panel shows a condition that violates the Metelli model because the RGB values of the overlay lead to chromaticities outside the RGB triangle and even beyond the spectral locus (not shown). Hence point V would have a negative B value, which is physically unrealizable [4, 5]. Figure 1 depicts a display for a condition corresponding to Fig. 2 (left) where the colors violate equations (2) and (3) of the Metelli model. In a laboratory setting, such violations are not unusual, suggesting that our perception of transparencies does not require a strict enforcement of the Metelli conditions.

2. Methods

Displays similar to Fig. 1 were generated on a G4 eMac computer. The R, G, B chromaticities were [{0.64, 0.33}, {0.28,, 0.60}, {0.15, 0.073}] with maximum screen luminance of 145 cd/m^2 as calibrated by LaCIE Blue eye and Monaco Optix instruments. The gamma was set at 1.0, and the illuminant was modeled as D65 (0.312, 0.329). The overall display subtended 18 x 18 cm and created a neutral gray background of luminance 48 cd/ m^2. Superimposed on this background were the two adjacent panels A and B, each 7.5 x 15 cm. On top of these panels was a 4 x 4 cm

overlay, split vertically into halves to create panels P and Q. The typical viewing distance was 60cm. (This was not a critical parameter.)

At the bottom of the display was a slider that could be moved by the subject to adjust the R,G,B values. In pilot studies, these values were set for each panel, enabling us to explore a wide range of conditions. During this series we observed several subjects who would accept partial transparencies when only one panel satisfied the Metelli conditions [6 – 12]. Hence, to avoid independent settings for P and Q, we linked the RGB values of the two halves of the overlay.

-Figure 3 about here -

Our setup is clarified in Fig. 3, which is part of a planar section in RGB space. This plane is defined by the RGB values of A, B, and the anchor point *max-PQ* . This last point is the most extreme RGB value for P,Q for the chosen task. Given points A,B we then located their mid-point, C. Now a line L_{pq} joining *max-PQ* with C (*mid-AB*) can be calculated. Twenty to thirty-five uniformly spaced RGB positions along the line L_{pq} were chosen, the number depending upon the experiment, ranging from *max-PQ* to *min-PQ* as illustrated in Fig. 3. From each of these positions, the two sets of RGB values were calculated, one for P, and the other for Q at an orientation parallel to AB. These values of P and Q were yoked to depart symmetrically from the line L_{pq}. The extent of the departure from L_{pq} was controlled by the subject using a slider visible at the bottom of the display. Hence, if the mid-PQ position was set at the position C on the line L_{pq}, the extreme P Q settings would be A and B. A similar procedure was used at all other points along line L_{pq} . Hence, at each of these points, the chromaticities of P and Q were pulled apart until the subject failed to see the PQ overlay as transparent. (Note that unlike the anchor point *max-PQ*, over most of the interior region of the parallelogram, it is possible to pull P,Q apart so their RGB positions lie outside the parallelogram.) The P-Q separation was then reduced until the percept of transparency reappears, and this setting was

entered into a data file as the transparency limit for that trial. The result is a set of PQ values that construct (curved) loci analogous to the AV and BV rays shown in Fig. 2. These loci were stored as the responses.

During each trial, there was also a calculation that determined whether any of the R,G,B beam values were inadvertently being frozen at their maximum levels. A signal light indicated when such clipping occurred, and these settings were replaced by the limiting values just inside the clipping.

3. Analysis

3.1 Metelli Limits

The response files contained the set of RGB values for P and Q, as well as the inferred reflectance α_λ and transmittance τ_λ, as calculated from equations 1. (Summaries are given in Appendix A, showing the RGB values for A,B and P,Q for some of the more important violations.) To simplify the analysis, the data for each trial were typically plotted in rank order on the [0,1] interval with *min-PQ* =0 at the left end of the scale, and *max-PQ* =1 at the right end. For most cases, these extreme values for transmittance and reflectance are pinned at 0 or 1 by this construction, and are the expected limiting values. Fig 4 shows example plots for one condition where only the B values were varied by the subject. (The RGB parameters were A = {0.5, 0.5, 0.7), B = {0.5, 0.5, 0.3}, and *max-PQ*={1, 1, 1 }, as shown in row 1 of the Table in Appendix A). The upper plot gives the value of the inferred Blue coordinate of the overlay needed to satisfy the Metelli transmittance condition, whereas the lower plot shows the result for inferred reflectance. Note there is a regular pattern with almost half the points requiring non-physical values for either transmittance or reflectance. However, the regions of the violations are different for each, as will be discussed shortly.

- Figure 4 about here -

To clarify the different perceptions of the overlay, we have indicated by vertical dashed lines three slices L, M and H, which are mnemonics for "lower", "middle" and "high" values for PQ. Slice M corresponds to the trial position where the PQ overlay has RGB values midway between those for A and B. Hence by adjustment of the slider, P and Q can respectively match A and B. Ideally, we expect that at *mid-PQ* the extreme settings should be A and B with τ_λ = 1.0 and the inferred reflectance α_λ equal to the average of A and B. However, this condition is an obvious singularity. Although the extremes for τ_λ are typically greater than one in this region, we sometimes find a dip in transmittance back toward 1 near *mid-PQ* = 0.5 (line M in Fig. 4).

A second, and more interesting type of singularity appears near the lower and higher regions of the reflectance calculation indicated by the lines L and H in Figure 4. These lines correspond to PQ values of 1/3 and 2/3. Note that to the left of L and to the right of H, we have violations in α_λ, with high variance near L and H. Both slices correspond to a change in the sign relationships between the denominator and the numerator of equation (3). For the illustrative example, the value of (A-B) is fixed over all trials, but the P-Q difference increases as the overlay changes from dark tones, through gray, to white. Near both L and H these differences are numerically similar to the A-B difference. Data points near these singularities had high variance, and values that exceeded 1.5 or were less than –0.7 are plotted on the panel boundary.

One might argue that both the L and H violations are simply due to noise in the observer's settings, and hence are not significant. However, the pattern of three negatively sloped loci about the L and H singularities reveal an underlying regularity that clearly is not just noise. Furthermore, note that if we consider both transmittance and reflectance together, the Metelli violations occur over the full range explored, not just in the L and H regions. The

reflectance violations α_λ are when the overlay has a blackish or whitish tint, whereas the transmittance τ_λ violations are when the overlay appears grayish. Clearly, there is a real effect here.

Of passing interest are the loci for both α_λ and τ_λ if they are simultaneously satisfied and follow the boundary of the A, *max-PQ,* B*, min-PQ* parallelogram illustrated in Fig. 2. The dashed curves in Fig. 4 show this constraint, relaxed slightly for α_λ. For transmittance, all points lie on a triangle with the reflectance of 1 at *mid-PQ* =0.5 and are zero at both *max* and *min PQ*. For reflectance, the limiting locus is a step from 0 to 1 at *mid-PQ*. In the figure, this locus is rounded to create an ogive, which better reflects plausible observer settings.

3.2 Kubelka Munk Limits

The Metelli model assumes that the fraction τ_λ of light coming off the background is transmitted through the overlay without internal scatter. A more realistic physical model is to include effects of all light scattered internally off the opaque particles of the overlay. In this vein there have been several analyses of optical conditions such as haze or fog, or filters with internal reflections, etc. that indicate the Metelli model, although very simple, is a good approximation for other transparency effects [13 – 17]. To add to this list, we have calculated the equations for inferring physical absorbance and turbitity transmittances, according to the Kubelka-Munk model [4, 18, 19]. Appendix A includes the results of these calculations for some of our trials. As others have found before us, the limiting conditions for the more physically realistic models were rather similar to Metelli's. Hence when a Metelli violation occurred, typically that setting also violated the Kubelka-Munk model (see also [20].) The intuitive explanation for the similar results is that

sign shifts in the contrast difference between P and Q and A and B usually do not survive either model.

4. Results: Conditions for Imaginary Colors

Perceptual violations of any physical model can be the result of an inadequate model, or alternatively, a failure in perceptual inference, or both. A few simple examples, together with informal observations, show that most of the violations we observe are the result of non-veridical perceptual inferences as well as inadequate physical models for configurations of opaque and turbid layers.

4.1 Independence of R,G,B

Models for transparency, such as Metelli's, that ignore fluorescence, imply that light from any spectral region will act independently of light from another spectral region. In contrast, an observer's color channels may interact, such as when they are combined for brightness estimates, or in a color-opponent representation. To test for the independence of the RBG values, let us keep the blue values of A and B as before in Fig 4, but shift the colors of A and B either toward the red or to the green. Similarly shift the max-PQ value (i.e. the original {1, 1, 1} values) by a similar amount. (In the red-shifted case the new max-PQ values will be {1, 0.7, 0.7} and the upper limit for the blue channel will be 0.7.) Such a lateral shift in the RGB space does not affect the conditions on τ_λ and add a mild constant to α_λ. Hence the result shown in the upper panel of Fig 4 should be unchanged, whereas the lower panel will change by a vertical shift. (This claim is easily checked by referring to equations (2) and (3).)

Five subjects previously run on Task 8, were run on this new Task 21 (see Appendix A.) Although the results of some of these observers exhibited three negatively sloped regions as seen on the earlier on the earlier task (i.e. the pattern in Fig. 4), the averaged data for all of the subjects used for

Task 21 had extremely high variance. This was most pronounced on the inferred reflectance. Further inspection of individual data revealed that the high variance results resulted from averaging over two quite distinctive patterns. These individual differences are exhibited in Fig.5.

Two of the five subjects had patterns for inferred transmittance and reflectance similar to that of Fig. 4, with inverted U-shaped loci for transmittance τ_λ and negatively sloped loci for reflectance α_λ. Their data are shown on the left two panels of Fig 5. For these subjects, the red-shift manipulation thus had little effect on the Blue channel other than the expected truncation above 0.7 on the PQ axis where no data points could be collected. We conclude that for these observers there was little or no interaction between the R,G and B channels.

-Figure 5 about here -

In contrast, however, three of the five subjects had changes that were not expected. As shown in the right panels of Fig. 5, these new patterns appeared in both the inferred transmittance, and especially in the inferred reflectance. For these observers, the transmittance (top right) now falls within the acceptable 0 – 1 interval, as do most of the reflectance values (lower right), excepting where the overlay has a very dark color (i.e. to the left of the vertical line L.) Excepting this lower quarter of the range, the inferred reflectance increases almost monotonically to reach 1 at the extreme P,Q anchor point. This is a dramatic change from Fig. 4 and shows that for some observers, there can be strong interactions between R or G and the B channel.

4.2 Role of Achromatic Axis

From the results of Fig. 5, which were based on a red shift from an achromatic locus, one might expect that for some observers, a blue-green shift in the opposite direction might again lead to two or more varieties of results. Hence Task 13 was introduced to shift the mean of *minPQ* and *maxPQ* toward the green (see Appendix A for settings.) Four observers previously run on Task

21 (Fig 5.), were run on Task 13. One of these was significantly different from the other three, with patterns resembling Task 8. For the remaining three observers, the shift of the display toward the green resulted in much less severe violations. Fig 6 shows their averaged results. On the top are the inferred transmittances, which are the same for all the R, G, B channels. On the bottom, the black dots show the G channel reflectances, whereas the white dots show those for the B channel. Note the very compressed dynamic range for the B channel, which is otherwise similar to the G channel. (The R channel is similarly compressed.) Now there is an almost linear progression in α_λ and we see the characteristic triangular form for transmittance, all lying well within the Metelli limits for all channels for this class of observer.

- Figure 6 about here -

The most significant difference between the conditions of Figs 5 and 6 is that in the first case, the PQ locus is roughly parallel to the achromatic (black-white) axis whereas in the second case the PQ axis is tilted to run from a dark purple through a greenish gray to end in a very light green. (Using the Munsell notation [4], A is a violet (5PB5/8), whereas B is a yellow-green (7GY7/7).) The consequence of the second manipulation is to reduce the perceptible achromatic tint (e.g. blackish, grayish, whitish.) This observation, in addition to the markedly reduced violations seen for the same three subjects for the Fig 5 (right) condition, suggests to us that an achromatic channel plays a role in the inference of transparency –at least for some observers.

4.3 Perceived Depth of Overlay

Laboratory set-ups have reduced constraints as compared with real-world conditions. A consequence is the conventional Metelli configuration illustrated in Fig 1 and used here has a very large number of categorically different interpretations [7, 20 – 25]. For example, as mentioned, either P or Q may appear transparent, but not both (we instructed our subjects to

consider this a violation.) But more extreme, PQ can appear as a surface behind a window in A and B. Surprisingly, many of our subjects could not see – or NEVER saw this condition, whereas others rejected this percept as an acceptable transparency (because we specifically stated that PQ were to appear as an overlay.) One of our eight subjects was known to be stereo-anomalous [26, 27], with reduced ability to process uncrossed disparities. Extensive studies with this subject confirmed that the extreme violations of the Metelli condition, including those for Fig 5 (left), typically occurred when others rejected PQ as lying behind, not in front of AB.

We also note that some observers can key in on different color channels, and this attention variable can affect the results. For example, if those channels become the dominant attribute of a surface behind the window, this percept can be ignored (both JJK and WR could easily perform this manipulation.) However, if the discrimination is absent, such as in a color anomalous observer, for example, that channel may contribute to the inference of an overlay, where it would otherwise be rejected. This attention factor further increases the complexity of the transparency percept and must be considered when counting the number of categorically different transparency interpretations for the observed PQ vs AB depth relations for each colored layer.

5. Discussion

Although the failure of simple physics-based models to account for transparency perception have been noted before [5, 9, 28 –31], our observations document some of their important characteristics. First, there are significant individual differences. Second, although we know the violations occur in either inferred transmittance or reflectance, both types of violations typically do not occur simultaneously. Thirdly, the achromatic axis appears to play a special role. (Based on other evidence, this suggestion has also been made by others [11, 22, 32 – 35]. Finally, we

note that the Metelli failures imply the inference of colors that are non-realizable and are, in that sense, imaginary.

Why observers accept certain non-physical conditions as transparent is not entirely clear. One explanation is to note that, unlike achromatic Metelli configurations, the perception of colored transparency will involve several chromatic channels in the visual system. Hence a simple hypothesis is that if one (perhaps more) of these channels have a violation but a weak signal and the remaining channels have strong signals and satisfy the Metelli conditions, then the observer will accept the overlay as transparent. Indeed, many of our results are consistent with a version of this hypothesis. For example, if observers differ in the proportion of active channels that exhibit violations, this hypothesis could explain the observer differences in Task 21 shown in Fig. 5. (See also Appendix B.) A related possibility is that observers might require different thresholds for what they consider acceptable signals in each channel. The effect of such a threshold will become very apparent if the contrast of the display is reduced. Then violations are more likely because the judgments are difficult, with the PQ separation much more difficult to notice. On the other hand, in the opposite case where the signals of all channels are raised to comparable levels, violations are expected to be much less frequent. Especially if the display is roughly equiluminant, for then the contrasts between regions in the red or green channels will be weak, but the blue channel can be boosted without affecting equiluminance. In this case the violations are minimal, and are confined to the PQ extremes.

The hypothesis that strong signals in channels that satisfy the Metelli conditions will dominate the violations in channels with weaker signals raises the question of how many channels are sufficient to produce the appearance of transparency. If the percepts are based on the analogs of the R,G,B channels, then we expect three channels to be in play. However, if

transparency perception is based on an opponent-color system, then the channels take a different form, such as Y-B, R-G, K-W. In this formulation, the K-W achromatic channel plays an explicit role, which is not the case for RBG. In addition, excepting the equiluminance case, Appendix C shows that the Metelli conditions cannot be verified for Y-B and R-G. But it can be shown that if Metelli violations occur in any one of the RGB channels, then there is a 99% certainty that there is a violation in the luminance or achromatic channel. This means that, in almost all cases, for the opponent-color system *only* the achromatic channel needs to be checked for Metelli violations.

Let us suppose, however, that observers used an opponent process scheme to judge transparencies (and hence did not ignore the chromatic Y-B, R-G channels.) In this case, violations can be introduced (such as in Task 8.) For example, observers may not always ignore the Y-B, R-G channels and may add chromatic content to the display to create a hint of the background to the overlay [9, 30]. Then violations resulting from adding chromatic content will have the greatest effect in the presence of strong achromatic signals, namely when the percept is of a black to dark gray or the complementary percept of light gray to white, as seen in Figs. 4, 5.

Curiously, when the display is equiluminant, adding tints of the background to the overly can lead to physically plausible transparencies using an opponent-process scheme. First, note that in this case, the achromatic channel conveys no significant information about the overlay. Hence the Metelli transparency can be decided on the basis of whichever opponent channel carries the significant structural information. As shown in Appendix D, the condition is that the opponent channels should have equal sign and that the contrast in the overlay should be lower than that in the background.

In sum, although we favor the hypothesis that observers use an opponent process scheme for judging transparency, we have no conclusive proof that this is the case. The striking

differences among observers also presents a problem: do some observers rely more on the achromatic channels than others? Or are all observers using an opponent-process scheme, with some invoking the chromatic channels in non-equiluminant conditions when others do not?

Our final comment re-addresses the main claim, namely that violations of the Metelli conditions (or the Kubelka-Munk model [18]) can easily be created in chromatic displays. This does not imply that most inferences about transparency in the real world will be flawed. First, many additional constraints come into play, and these typically augment the reduced conditions created in the laboratory. Secondly, perhaps more important, is that the violations reported here assume the Metelli model of a homogeneous overlaid turbid layer. However, analogous situations appear in the natural world that are created in other ways. For example, consider the occluding contour of neighboring surfaces where a shadow is cast across the boundary. This "x-junction" has the same form as the junction formed between the P, Q, A, B regions of Fig. 1 and certainly plays a major role [28,32]. But the model will be quite different because in this case the scattering is absent, like a clear overlay without turbidity. Another common configuration that has the same appearance as the panels in Fig. 1 would be if the interior square is a hole, with surfaces P, Q lying behind A, B. Then again, the Metelli model is not appropriate. In fact there are four conditions of this kind that correspond to the placement of the plane of the transparent surface [20]. In our experiments, although many observers consistently saw the PQ panels as in front of AB; others observed cases where PQ appeared as a hazy film behind AB. Their settings may have been appropriate for this interpretation. Hence depth assertions also can influence judgments of transparency, and may help distinguish between related phenomena such as translucency, fluorescence , or shadows [25]. Simply put, there are a variety of physical phenomena with many distinctive underlying parameters; we cannot expect a system with

limited, reduced stimuli to categorize all these phenomena reliably. Understanding perceptual transparency in a real world setting will require a much more complex model than Metelli's, namely one that considers the Gestalt associated with a host of possible physical interpretations that include spatial configurations, their depth relationships, how they are illuminated as well as the chromatic content of the display [20].

A. Appendix: Table of Experimental Parameters and Violations

The task number, *maxPQ* and {A,B} settings are shown in the first three columns. (Note that the latter two values fully specify the task.) In the remaining columns, we list some representative violations, but not necessarily the extremes for α_λ and/or τ_λ. For example, from the plots of Fig 4, we picked trial 9 for transmittance, and trials 4 and 16 for reflectance for the blue channel.

Task#	max-PQ	{A, B }	Pos#	{ τ_λ , α_λ }	Metelli Violation (PQ)	Comment
8	{1.0, 1.0, 1.0}	{0.5, 0.5, 0.7}	[4]	{0.75, -0.6}	{0.15, 0.15, 0.26}	K-M violation
		{0.5, 0.5, 0.3}			{0.15, 0.15, 0.04}	
			[9]	{1.2, 0.7}	{0.4, 0.4, 0.60}	K-M violation
					{0.4, 0.4, 0.18}	
			[16]	{0.9, -5.0}	{0.75, 0.75, 0.95}	K-M violation
					{0.75, 0.75, 0.54}	
13	{0.4, 1.0, 0.4}	{0.2, 0.3, 0.7}	[16]	{0.85, -0.3}	{0.20, 0.24, 0.64}	
		{0.5, 1.0, 0.01}			{0.46, 0.85, .04}	few violations
20	{0.8, 1.0, 1.0}	{0.2, 0.5, 0.7}	[6]	{1.1, -0.8}	{0.32, 0.6, 0.82}	
		{0.2, 0.5, 0.3}			{0.32, 0.6, 0.38}	K-M violation
			[7]	{1.05, -2.0}	{0.38, 0.65, 0.86}	
					{0.32, 0.6, 0.38}	K-M violation
21	{1.0, 0.7, 0.7}	{0.8, 0.5, 0.7}	[8]	{0.8, -0.8}	{0.46, 0.16, 0.31}	red shifted task #8
		{0.8, 0.5, 0. 3}			{0.46, 0.16, .012}	
29	{0.56, 0.56, .01}	{0.48, 0.44, 0.80}	[17]	{0.5, 1.1}	{0.54,0.53, 0.19}	equiluminance
		{0.53, 0.56,021}			{0.545, 0.548, 0.12}	minor violation
31	{1.0, 1.0, 1.0}	{0.3, 0.7, 0.7}	[18]	{0.65, 1.7}	{0.71, 0.99, 0.99}	K-M violation
		{0.7, 0.3, 0.3}			{0.99, 0.71, 0.71}	
32	{0.7, 0.7, 1.0}	{0.3, 0.7, 1.0}	[24]	{0.85, 1.03}	{0.27, 0.69, 0.99}	blue shift #31
		{0.7, 0.3, 0.6}			{0.70, 0.27, 0.57}	minor violation

B. Appendix: The independence of spectral sub-channels

Consider a system made up of two non-overlapping spectral sub-channels. Suppose the Metelli transparency conditions are checked for each channel separately. Moreover, suppose these conditions are also checked for the super-channel formed by merging the two sub-channels. This might happen in a system with two spectrally selective channels in which an "achromatic channel" was formed at a secondary stage, the sub-channels being of a primary (retinal) stage. Then an important question is: If the Metelli conditions are satisfied at the sub-channel stage, can they ever be violated at the secondary stage, that is for the super-channel?

The answer would be immediate if the Metelli conditions would be linear. For instance a "luminance" signal could be computed at the sub-channels and the luminance computed for the super-channel would simply be the sum of these two luminances. Thus equality of luminance could be checked either at the primary level (adding the two outcomes) or at the secondary level; it makes no difference. In the Metelli transparency case, which is non-linear, it is feasible that the conditions are satisfied in both sub-channels, but are violated for the super-channel. Although the Metelli constraints are only mildly non-linear (the dividing surfaces in parameter space being either planar or ruled surfaces) this condition still has to be analyzed.

Consider again the Metelli conditions for transparency in the case of two background areas A and B, that appear as two different colors behind a single transparent overlay, say P and Q, where P is A as seen through the overlay and Q is B as seen through the overlay (i.e. Fig. 1). The condition is

$$\begin{aligned} F(A,B;P,Q) = (((P>Q)\wedge(A>B))\wedge((((Q+A+PB)>(P+QA+B))\wedge(P>A)) \\ \vee((P<A)\wedge(PB<QA))))\vee((P<Q)\wedge(A<B)\wedge \\ (((PB>QA)\wedge(P<A))\vee((P<A)\wedge(Q+A+PB)<(AB+QA+B))))). \end{aligned} \tag{B1}$$

For the two sub-bands 1, 2 we write

$$C_1 = F(A_1, B_1; P_1, Q_1)$$
$$C_2 = F(A_2, B_2; P_2, Q_2) \qquad \text{(B2)}$$

and for the super-channel

$$C_{1+2} = F(\frac{(A_1 + A_2)}{2}, \frac{(B_1 + B_2)}{2}; \frac{(P_1 + P_2)}{2}, \frac{(Q_1 + Q_2)}{2}) \qquad \text{(B3)}$$

where we divide by two to keep the values within the [0,1] range. Then

$$H = (C_1 \wedge C_2) \wedge \neg C_{1+2} \qquad \text{(B4)}$$

expresses the violation of the Metelli transparency condition for the super-channel when the conditions are satisfied in both sub-channels. Algebraic simplification (done via Mathematica) yields a very long expression (16 lines) that conceivably might still be identically TRUE. In order to decide the issue we evaluated the expression for random values of the parameters, where A, B, P, and Q for either channel were drawn from a uniform distribution on [0,1].

We find that in about 1% of the cases the expression evaluates to TRUE, in 99% of the cases to FALSE.

Thus when the Metelli conditions are satisfied in the sub-channels there is indeed no *guarantee* that they might not be violated in the super-channel, though this will happen only in *rare cases*. For the purposes of the present work it is safe to ignore such rare occurrences.

In case Metelli is not violated in the super-channel, it is still possible that there is a violation in one or both of the sub-channels. From a simulation of a 100,000 cases we estimate approximate frequencies of occurrence as follows (the sequence is sub-channel A, sub-channel B, super-channel, "T" stands for TRUE (i.e. Metelli constraints satisfied), "F" for FALSE (Metelli constraints violated):

FFF	58.6%
FFT, TFF, FTF	10.6%

FTT, TFT	3.34%
TTF	0.896%
TTT	1.90%

All combinations occur, though with very different frequencies. Apparently, acceptance of transparency in the super-channel by no means implies absence of violation in the sub-channels.

Notice that the trichromatic case is not essentially different from the dichromatic case considered here.

C. Appendix: The Metelli conditions in an opponent color system

Consider the simple case of a dichromatic opponent system. Spectral sub-band channels X and Y (say) are encoded as U=(X+Y)/2, that is the "achromatic channel", and V=(X-Y)/2, that is the "opponent channel". When X, Y are on [0,1], then U, V are again in [0,1], whereas the opponent signals vary on [-1/2, +1/2].

We write the background areas A and B as (K+L)/2 and (K-L)/2 respectively, where K denotes an "achromatic" and L an "opponent" channel. Likewise, we write the areas P and Q (that are the backgrounds A and B as seen through the transparent overlay) as (S+T)/2 and (S-T)/2 respectively, where S denotes an "achromatic" and T an "opponent" channel. The Metelli condition can thus be expressed as (see Appendix B):

$$F(\frac{K+L}{2},\frac{K-L}{2};\frac{S+T}{2},\frac{S-T}{2}). \qquad \text{(C1)}$$

This inevitably leads to a rather complicated expression. However, it can be simplified considerably, and without sacrificing generality, by considering suitable special cases. Consider the case $A > B$. It is still general, for if $A < B$ then we simply mirror reflect the Metelli configuration. Now $A > B$ implies $P > Q$ when Metelli transparency is to be possible, so we may assume both $A > B$ and $P > Q$ here. Then the expression simplifies to $(KT < LS)$, which we prefer to write as

$$\frac{L}{K} > \frac{T}{S}, \qquad \text{(C2)}$$

in which ratios of the opponent to the corresponding achromatic channels are compared. But this implies that the Metelli transparency conditions cannot be expressed in a form

$$G(K,S) \wedge H(L,T), \qquad \text{(C3)}$$

where $G(K,S)$ is a constraint in terms of the achromatic, and $H(L,T)$ an independent constraint in terms of the chromatic signals.

Thus one cannot have a system that checks for Metelli consistency in independent achromatic and opponent channels and subsequently combines the results by a logical AND. In order to check Metelli transparency one needs to consider the achromatic and opponent channels *simultaneously*, essentially back transforming to the primary intensity (non-opponent) channels.

To summarize, for the case of a true opponent system one expects Metelli transparency to be a function of the achromatic channel only, the opponent channels merely contributing to the "mental paint".

This analysis applies equally well to the trichromatic case.

D. Appendix: Equiluminant configurations

Notice that for the *equiluminant* case, i.e. when K==S (Appendix C), there is a very simple condition. That is to say, if the configuration is *known* to be equiluminant (which would be signaled by the absence of contrast in the achromatic channel), Metelli transparency can be decided on the basis of the opponent channel (which is the only channel carrying significant structural information in that case). This condition is that the opponent channels should have equal sign and that the contrast in the overlay should be lower than that in the background, thus

$$(LT > 0) \wedge (|T| < |L|). \qquad \text{(D1)}$$

This strategy for deciding transparency is among the simplest, but applies only in roughly equiluminant displays. Note that these include strongly colored patterns.

References

1. F. Metelli, An algebraic development of the theory of transparency. Ergonomics **13** (1), 59-66 (1970).

2. F. Metelli, The perception of transparency. Sci. Amer. **230** (4) 90 – 98 (1974a).

3. F. Metelli, Achromatic color conditions in the perception of transparency. Pp 96 – 116. In R B MacLeod & H L Pick (eds) "Perceptions: Essays in honor of J J. Gibson." Cornell Univ. Press (1974b).

4. G. Wysecki & W. S. Stiles, "Color Science", Wiley: New York (1967).

5. W. Richards & A. Witkin, Transparency. Part II in Efficient Computations and Representations of Visible Surfaces, W. Richards & K. Stevens; Final Report AFOSR Contract 79-0020, pp 46 – 72. MIT Artificial Intelligence Laboratory (1979).

6. F. Metelli, S. C. Masin, M. Manganelli. Partial transparency. Attidell' accademie Patavina di Scienze Lettere ed Arti **92**, 115-169, (1981).

7. J. Beck, & R. Ivry, On the role of figural organization in perceptual transparency. Perception & Psychophysics **44**, 585 – 594 (1988).

8. F. Metelli, O. da Pos, & A. Cavedon, Balanced and unbalanced, complete and partial transparency. Percept. & Psychophys. **38**, 354 – 366 (1985).

9. O. da Pos, "Trasparenze", Padua, Icone (1989).

10. T. Kozaki, M. Fukuda, Y. Nakano, N. Masuda. Phenomenal transparency and other related phenomena. Hiyoshi Rev. of Natural Science (Keio University) **6**, 68 – 81 (1989.)

11. M. Fukuda & S. C. Masin, Test of balanced transparency. Perception **23**, 37– 43 (1994).

12. S. Masin, The luminance conditions for transparency. Perception **26**, 39 – 50 (1997).

13. J. Beck, Additive and subtractive mixture in color transparency. Perception & Psychophysics **23**, 265– 267 (1978).

14. W. Gerbino, C. I. Stultiens, J. M. Troost & C. M. de Weert, Transparent Layer Constancy. Jrl. Expt'l Psych.: Human Percept. & Performance, **16**, 3- 20 (1990).

15. F. Faul, & V. Ekroll, Psychophysical model of chromatic perceptual transparency based on subtractive color mixture. J. Opt. Soc. Am. A **19** (6), 1084 – 1095 (2002).

16. S. Nakauchi, P. Silfsten, J. Parkkinen & S. Ussui, Computational theory of color transparency: recovery of spectral properties for overlapping surfaces. Jr. Opt. Soc. Am. A, **16**, 2612 – 2624 (1999).

17. J. Hagedorn & M. D'Zmura, Color appearance of surfaces viewed through fog. Perception. **29**(10), 1169-1184 (2000).

18. P. Kubelka & F. Munk, Ein Beitrag zur Optik des Farbenstriche. Z. techn. Physik **12**, 593 (1934).

19. P. Kubelka, New contributions to the optics of intensely light-scattering materials, Part II. Non-homogeneous layers. J. Opt. Soc. Am. **44**, 330 (1954).

20. J. Koenderink, A. van Doorn, S. Pont, W. Richards. Gestalt and Phenomenal Transparency, J. Opt. Soc. A. A **25**, 190-202 (2008).

21. W. Metzger, Ueber Durchsichtigkeits-Erscheinungen. Rivista di Psicologia. Fascicolo Giubilare **49**, 187-189 (1955.)

22. K. Nakayama, S. Shimojo & V. S. Ramachandran, Transparency: relations to depth, subjective contours, luminance and neon color spreading. Perception **19**, 497 – 513 (1990).

23. Nakayama, K. & Shimojo, S. Experiencing and perceiving visual surfaces. Science **257**, 1357 – 1363, (1992).

24. M. Singh & D. D. Hoffman. Part boundaries alter the perception of transparency. Psychol. Science **9**, 370 –378 (1988).

25. M. Singh, & B. L. Anderson, Toward a perceptual theory of transparency. Psychol. Rev. **109**, 492 – 519 (2002).

26. W. Richards, Anomalous Stereoscopic Depth Perception, Jr. Opt. Soc. Am. **61**, 410-414 (1971).

27. R. Van Ee & W. Richards. A planar and volumetric test for stereoanomaly. Perception **31**, 51-64, 2002.

28. B. L. Anderson, A theory of illusory lightness and transparency in monocular and binocular images. Perception, **26**, 419 – 453 (1997)

29. V. J. Chen & M. D'Zmura, Test of a convergence model for color transparency perception. Perception **27**, 595-608 (1988).

30. M. D'Zmura , P. Colantoni , K. Knoblauch , B. Laget. Color transparency. Perception **26**(4), 471- 492 (1997).

31. M. Singh & B. Anderson, Photometric determinants of perceived transparency. Vision Research **46**, 879 – 894 (2006).

32. B. L. Anderson, The role of occlusion in the perception of depth, lightness and opacity. Psychol. Rev. **110**, 762 – 784 (2003).

33. M. Singh, & B. L. Anderson, Perceptual assignment of opacity to translucent surfaces: the role of image blur. Perception, **31**, 531 – 552 (2002).

34. J. Wolfe, R. Birnkrant, M. Kunar, T. Horowitz. Visual search for transparencies and opacity: attentional guidance by cue combination? Jrl. Of Vision **5**, 257-274 (2005.)

35. J. M. Fulvio, M. Singh & L. T. Maloney, Combining achromatic and chromatic cues to transparency. Jrl. of Vision, **6** (8):1 , 760 – 776 (2006).

Acknowledgements

This work was sponsored in part via the European program Visiontrain contract MRTNCT2004005439 to JJK, with support also provided to WR by AFOSR contract #6894705. Special thanks to SML for his participation in the experiments; his observations helped clarify our conclusions.

List of Figure Captions

Fig. 1. An example transparency. The R,G,B values are: A=={0.50, 0.50, 0.70}; B=={0.50, 0.50, 0.30}; P=={0.20, 0.20, 0.40) and Q=={0.20, 0.20, 0.05}. Using Metelli equations [1a,b], an reflectance and transmittance of the overlay can be calculated for each R,G,B channel. For this example, the inferred reflectance and transmittance for the B channel was respectively -0.63 and 0.73. The negative value indicates a Metelli violation requiring an imaginary spectral surface color (see Fig. 2.)

Fig.2 Slice at the RGB color space, showing a violation of the Metelli conditions (left), and another example that is physically realizable (right.)

Fig. 3. Depiction of the experimental conditions. The parallelogram is part of a plane in RGB space defined by the points A, B and an anchor point *max-PQ*. Points are chosen along the line through C joining *max-PQ* and *min-PQ*. The boundary of the parallelogram indicates the limiting PQ settings for the Metelli conditions. In the lower panel, we show averaged settings for Task 8 (Fig. 4.) Note that observers accept settings that lie outside the parallelogram.

Fig. 4. Averaged values of transmittance τ_λ (top) and reflectance α_λ (lower) for the upper bounds of transparency settings of 8 subjects, for Task 8 (see Table1.) The fine dashed lines indicate values if both of Metelli's conditions were met at the same time (the ideal step function for the lower panel has been smoothed slightly). The L and H vertical lines give approximate boundaries for grayish tones to the overlay (below L, very dark, above H, very light). Note that although reflectance is mostly within the [0,1] interval over the grayish range, most of the transmittances exceed one. Similarly, the reverse is true outside this gray interval. (Points greater

than 1.5 or less than –0.7 are plotted on the upper and lower boundaries of the panel. Arrows indicate very large values for standard deviations that exceeded the range indicated on the left.)

Fig. 5. Inferred transmittance (top) and reflectance (bottom) for task 21, where the PQ loci are shifted to the red. The left two panels are data from two subjects, the right panels are data from three subjects, all of whom provided similar data for task 8 (Fig. 4.) The PQ values of the overlay vary from pinkish to dark purple, with max-PQ = {1, 0.7, 0.7} . The background panels are A= {0.8, 0.5, 0.7}, B = { 0.8, 0.5, 0.3 }. See Appendix A for further details.

Fig. 6. Inferred transmittance (top) and reflectance (bottom) for task 13 for three subjects used also for task 21 (right panels of Fig. 5.) For task 13 the PQ loci are shifted away from the achromatic locus to the green. The PQ values of the overlaid region vary from light blue-green (5BG8/5) to red-purple (2.5RP3/8), moving through a greenish gray. max-PQ = {0.4, 1., 0.4}. The background panels are A= {0.2, 0.3, 0.7}, B = {0.5, 1., 0.01}. The transmittances for all three channels are the same; the white dots show the compressed reflectance values for the B channel; the black dots show G channel reflectance. See Appendix A and text for further details.

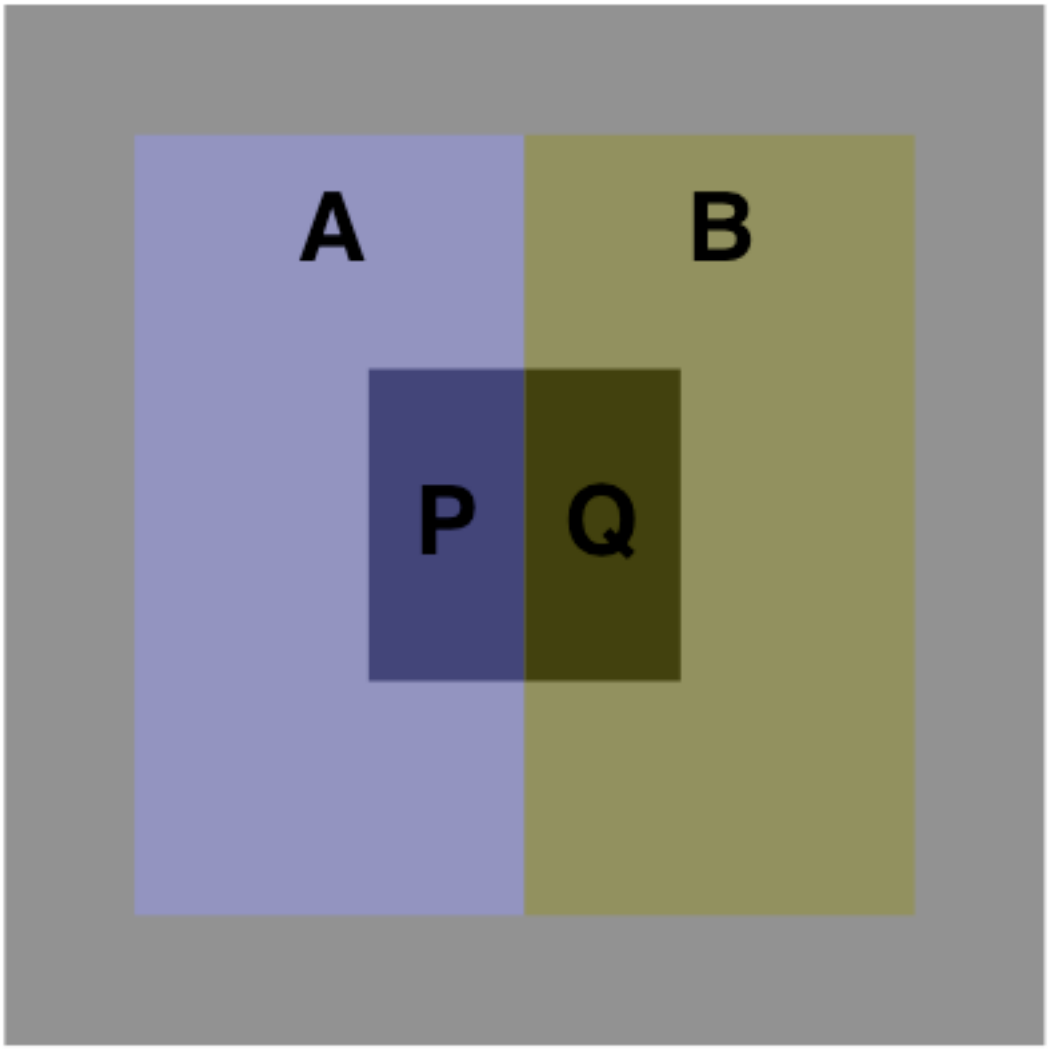

Fig. 1

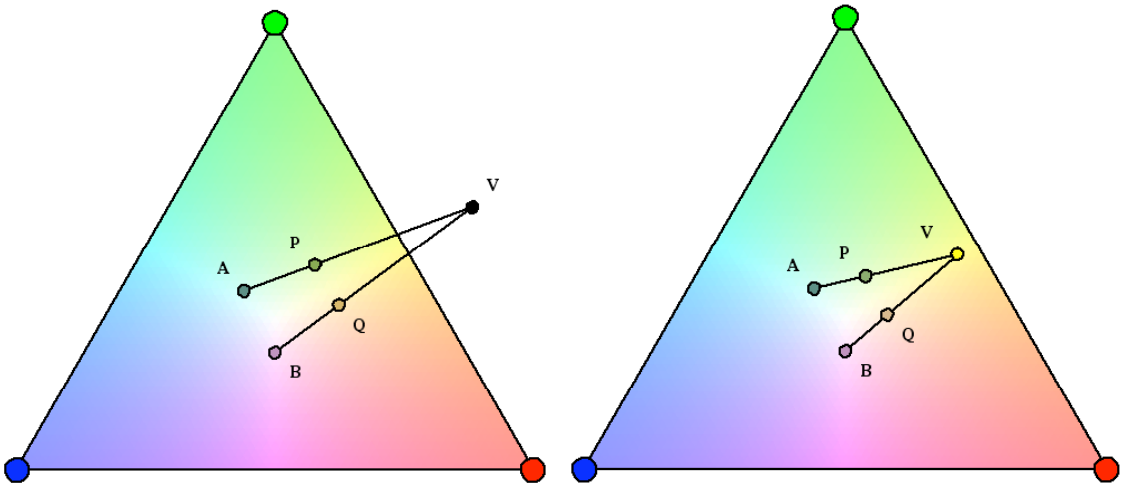

Fig. 2

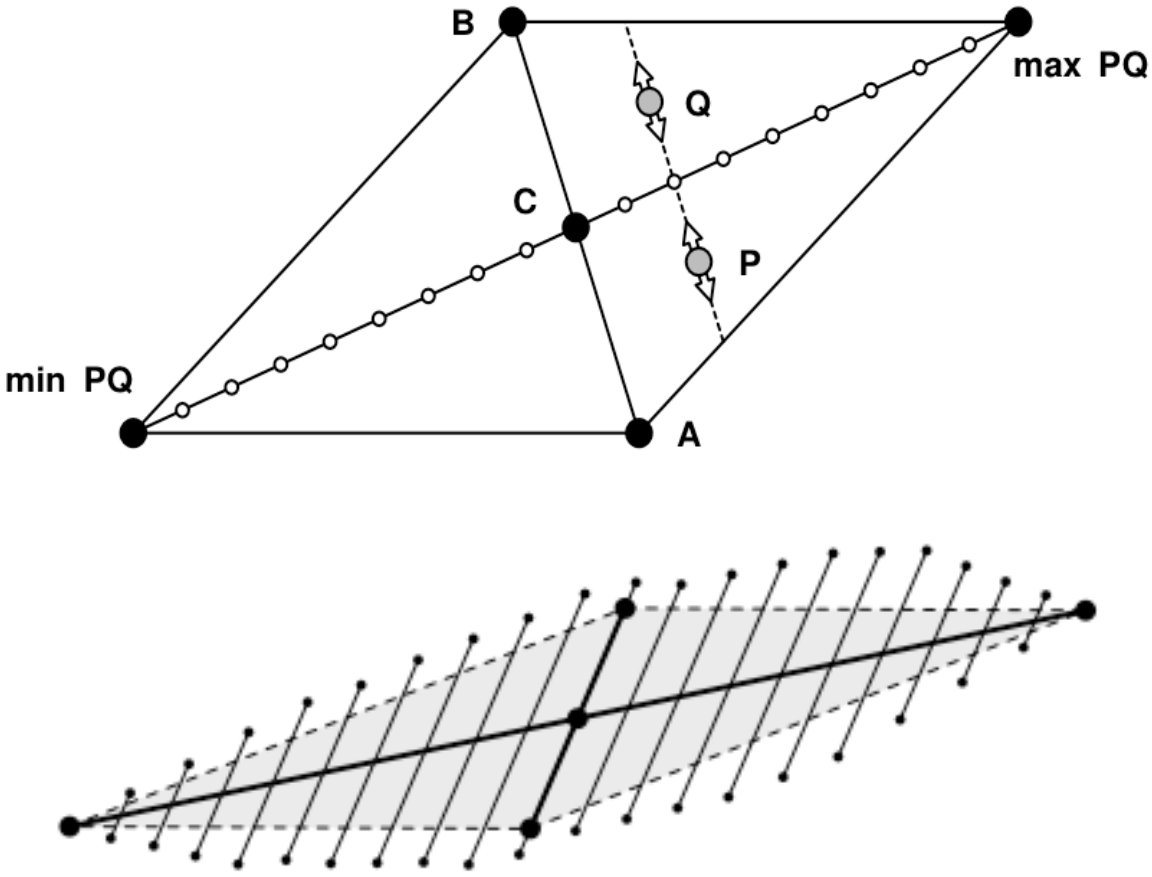

Fig. 3

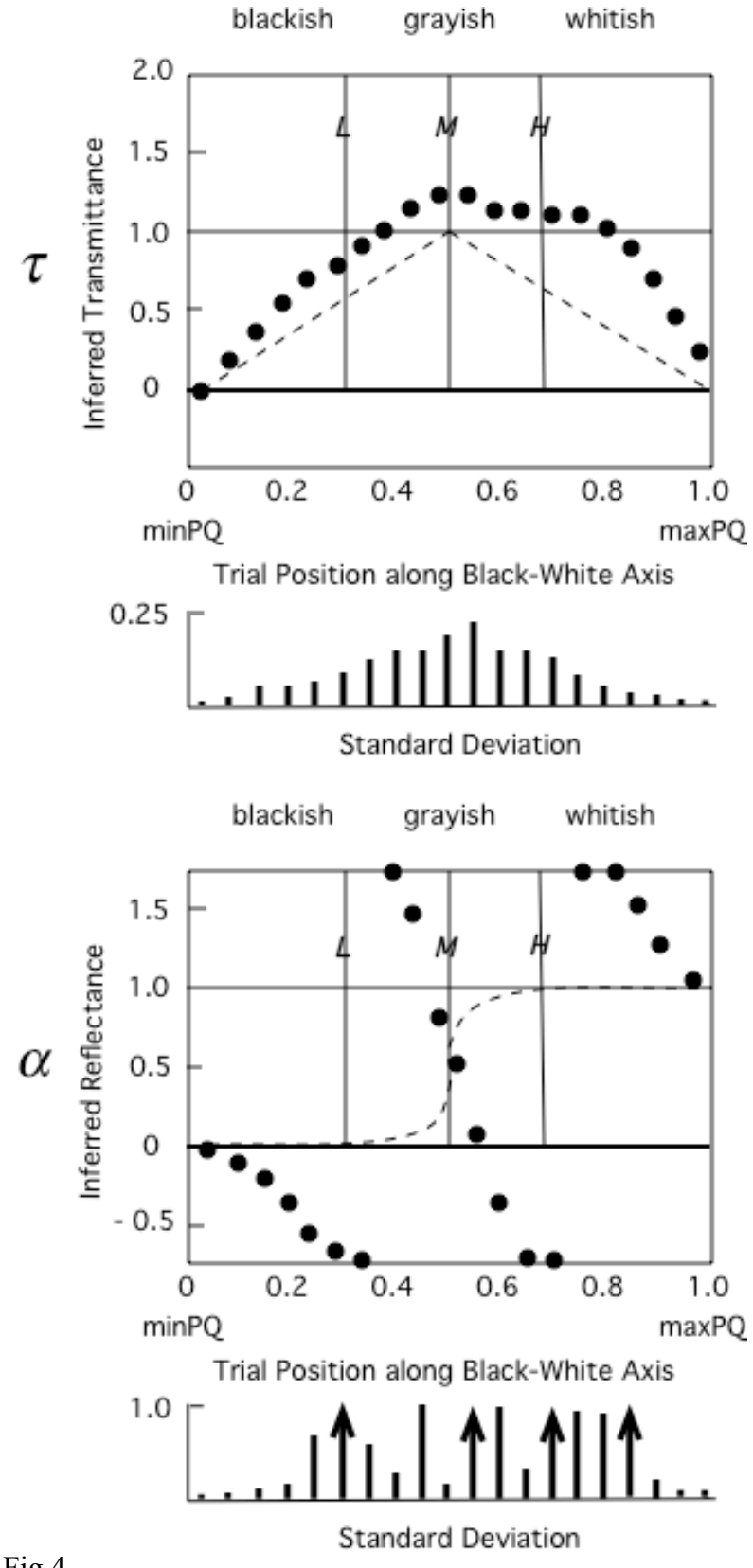
blackish
grayish
whitish
τ
Inferred Transmittance
2.0
1.5
1.0
0.5
0
L
M
H
0
0.2
0.4
0.6
0.8
1.0
minPQ
maxPQ
Trial Position along Black-White Axis
0.25
Standard Deviation
blackish
grayish
whitish
α
Inferred Reflectance
1.5
1.0
0.5
0
- 0.5
L
M
H
0
0.2
0.4
0.6
0.8
1.0
minPQ
maxPQ
Trial Position along Black-White Axis
1.0
Standard Deviation

Fig.4

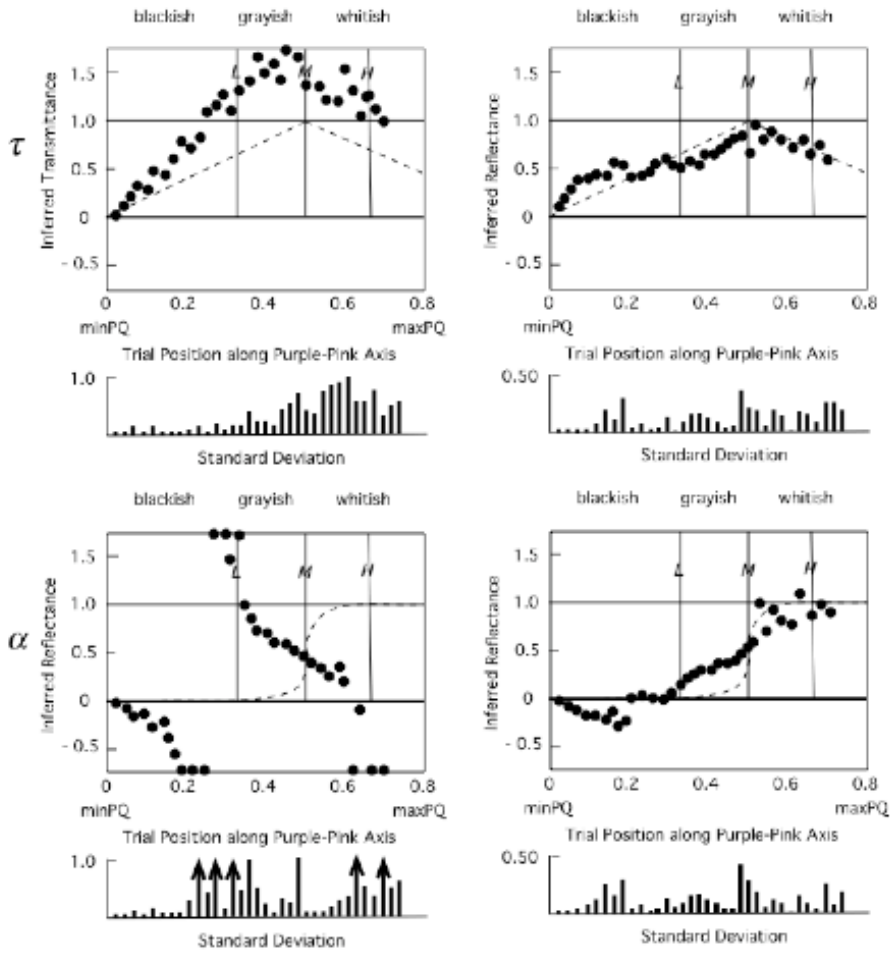
τ
α
blackish
grayish
whitish
L
M
H
Inferred Transmittance
Inferred Reflectance
1.5
1.0
0.5
0
- 0.5
0
0.2
0.4
0.6
0.8
minPQ
maxPQ
Trial Position along Purple-Pink Axis
1.0
0.50
Standard Deviation

Fig 5

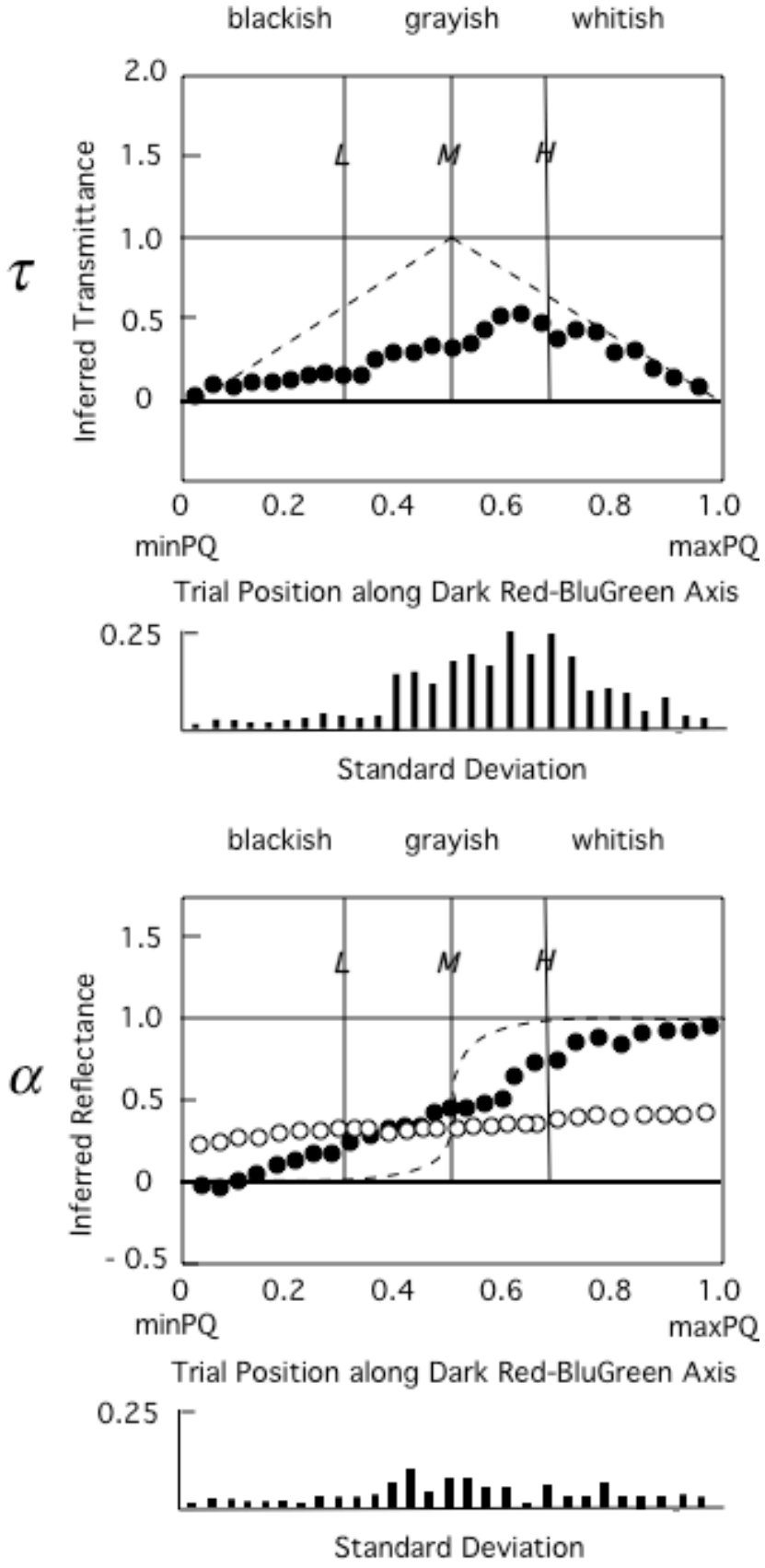
blackish
grayish
whitish
τ
2.0
1.5
1.0
0.5
0
L
M
H
Inferred Transmittance
0
0.2
0.4
0.6
0.8
1.0
minPQ
maxPQ
Trial Position along Dark Red-BluGreen Axis
0.25
Standard Deviation
blackish
grayish
whitish
α
1.5
1.0
0.5
0
- 0.5
L
M
H
Inferred Reflectance
0
0.2
0.4
0.6
0.8
1.0
minPQ
maxPQ
Trial Position along Dark Red-BluGreen Axis
0.25
Standard Deviation

Fig.6